Nrf2 Inhibits Periodontal Ligament Stem Cell Apoptosis under Excessive Oxidative Stress

Yanli Liu[1#], Hongxu Yang[2#], Yinhua Zhao[1], Min Zhang[1], Yongjin Chen[1*]**

[1] State Key Laboratory of Military Stomatology, Department of General Dentistry and Emergency, School of Stomatology, the Fourth Military Medical University, 145 Changle West Road, Xi'an, 710032, China

[2] State Key Laboratory of Military Stomatology, Department of Oral Anatomy and Physiology and TMD, School of Stomatology, the Fourth Military Medical University, 145 Changle West Road, Xi'an, 710032, China

[#]Theses authors contributed equally to this work.

[*] Corresponding Author: State Key Laboratory of Military Stomatology, Department of General Dentistry and Emergency, School of Stomatology, the Fourth Military Medical University, 145 Changle West Road, Xi'an, 710032, China

E-mail: cyj1229@fmmu.edu.cn

[**] Co-corresponding Author: State Key Laboratory of Military Stomatology, Department of General Dentistry and Emergency, School of Stomatology, the Fourth Military Medical University, 145 Changle West Road, Xi'an, 710032, China

E-mail: zhangmin@fmmu.edu.cn

Abstract: The present study aimed to analyze novel mechanisms underlying Nrf2-mediated anti-apoptosis in periodontal ligament stem cells (PDLSCs) in the periodontitis oxidative microenvironment. We created an oxidative stress model with H_2O_2-treated PDLSCs. Herein, we used real-time PCR, western blotting, TUNEL staining, fluorogenic assay and transfer genetics to confirm the degree of oxidative stress and apoptosis as well as the Nrf2 function. Surprisingly, we demonstrated that with up-regulated ROS and MDA levels, the effect of oxidative stress was obvious under H_2O_2 treatment. Anti-oxidative molecules were changed after the H_2O_2 exposure, whereby the anti-oxidative signaling of Nrf2 was activated with the increase of its downstream effectors, HO-1, NQO1 and γ-GCS. Additionally, the apoptosis levels gradually increased with oxidative stress and changes in the caspase-9, caspase-3, Bax and c-Fos levels, but not with caspase-8 and down-regulated Bcl-2. The enhanced antioxidant effect could not resist the occurrence of apoptosis. Furthermore, Nrf2 overexpression effectively improved the anti-oxidative levels and increased cell proliferation. At the same time, overexpression effectively restrained TUNEL staining and decreased the molecular levels of caspase-9, caspase-3, et al, but not that of caspase-8. By contrast, silencing the expression Nrf2 levels had the opposite effect. Collectively, Nrf2 alleviates PDLSCs via its effects on anti-oxidative and anti-intrinsic apoptosis by the activation of anti-oxidative enzymes.

Keywords: periodontitis; the periodontal ligament stem cells; the nuclear factor-erythroid 2-related factor 2; oxidative stress; apoptosis

Introduction

Periodontitis has become the third largest disease affecting human health after "cancer" and "cardiovascular disease", and it is also known as the leading killer in oral health [1]. Periodontal disease is a general term that is used to describe specific diseases that affect the gingiva and the supporting connective tissue and alveolar bone, which anchor the teeth in the jaws [2]. Currently, doctors recognize that the most important methods of curing periodontitis are sequential pre-treatment, such as eliminating local stimuli and plaque control, including foundation treatment, surgical treatment, repair and support treatment. However, the current tissue repair treatment methods are not desirable, which may be because of the lack of seed cells in tissue regeneration [3, 4]. In recent years, stem cell technology and the development of tissue engineering technology have brought new opportunities for repairing periodontal tissue defects. Some scholars, through animal experiments, have confirmed that mesenchymal stem cells (MSCs) with exogenous bone graft material composite for repairing periodontal tissue defects is better than single bone graft material repairs [4].

Periodontal ligament stem cells (PDLSCs) are a type of MSCs. Many studies have found that using PDLSCs to repair non-inflammatory alveolar bone defects works better than in repairing periodontitis bone defects [5]. Studies in recent years affirmed that local tissue generates in interleukine-8 (IL-8) and macrophage colony stimulating factor when inflammatory lesions occur in periodontal tissue. The generation of these two factors and complement activation exists in the periodontal beneath the epithelium and connective tissue from neutral polymorphonuclear leukocytes (PMNs) [6, 7]. PMNs act as the primary defense against outside microbial invasions, and after swallowing pathogens, their intracellular oxidase is activated, which absorbs a large amount of oxygen. PMNs produces reactive oxygen species (ROS), which is a strong antiseptic material that eliminates pathogenic microorganisms. It contains hydrogen peroxide (H_2O_2), ultra-oxygen anion, singlet oxygen, and free hydroxyls [8].

Oxidative stress (OS), which is mediated by ROS such as H_2O_2, plays a crucial role in the periodontitis. Sublethal concentrations of H_2O_2 can damage the body, directly or indirectly, by damaging cellular proteins, lipids, nucleic acids and other macromolecular substances that have physiological functions, which leads to low metabolic activity and cell cycle arrest by activating apoptosis [9, 10]. Apoptosis is a type of programmed cell death that is used to eliminate excess damaged or stressed cells throughout life in a variety of organisms, thus maintaining normal development, tissue remodeling and homeostasis [11]. Over the past decade, apoptosis has been identified as a critical factor responsible for PDLSCs damage and differentiation, and excessive OS can destroy their DNA through cell apoptosis [12]. OS is one of the biggest factors that influences stem cells. It can effect

PDLSC differentiation and even cause cell death [13].

It is well known that the nuclear factor-erythroid 2-related factor 2 (Nrf2) signaling pathway has an antioxidant effect and is involved in the cellular antioxidant defense system [14, 15]. Under normal conditions, Nrf2, combined with Kelch-like ECH-associated protein 1 (Keap1), exists in the cell. In response to OS, the cysteine residues of Keap1 are modified, which causes a conformational change that leads to the release Nrf2 and its phosphorylation. Additionally, this reduces the protein kinase recognition, increases the content and stability of Nrf2, and promotes its translocation into the nucleus. Nrf2 upregulates the expression of antioxidant and detoxifying genes by binding to antioxidant response elements (AREs) in the promoter region of the encoding genes, which starts the transcription of downstream target genes [16]. Research has confirmed that the phosphorylation of Nrf2 plays a main mechanistic role in oxidative stress resistance [17]. Nrf2/ARE activation, on the one hand, may inhibit pro-inflammation, including cytokines, inflammatory chemokines, cell adhesion factors, matrix metalloproteinases, 2 ring oxidase (cox-2) and inducible nitric oxide synthase (iNOS) [18,19]. On the other hand, it can increase a variety of downstream phase II detoxifying enzymes and antioxidant gene expression, including Heme oxygenase-1 (HO-1), CAT, SOD, gamma-glutamyl cysteine synthetase (γ-GCS) and NAD(P)H: quinone oxidoreductase 1(NQO1) [20-23].

To date, the role of Nrf2 in the occurrence and development of periodontitis is still unclear. Considering the above problems and combining the research previous experimental results, we have formulated the following hypothesis: the periodontitis local oxidative stress microenvironment can lead to PDLSC oxidation imbalance, which can accelerate their apoptosis and influence their repair regeneration function, and endogenous antioxidant molecules such as Nrf2 may play an important role in the process of this disease. The purpose of this study was to examine novel mechanisms of Nrf2-mediated anti-apoptosis in PDLSCs in the OS microenvironment.

Results

1. Culture and identification of PDLSCs

After culturing the PDLSCs, irregular patterns were found in the third-generation PDLSCs, mostly in their long spindle-like morphology. Through toluidine blue staining or osteogenesis and adipogenesis evaluations, all of the PDLSCs exhibited an ability to form colonies or transdifferentiate into osteogenic and adipogenic lineages (Figure 1A, B and C). RT-PCR results indicated that under osteogenic culture conditions, PDLSCs expressed higher levels of osteogenesis-related genes than found in the control medium after 21 days inducible, such as *BSP*, *OCN* and *ALP* (Figure 1D). At the same time, the adipogenesis-related genes *LPL* and *PPARγ* were expressed at higher levels in the adipogenic inducible condition than in the control medium after 14 days (Figure 1E). These passage three cells also had a strong proliferation ability, as demonstrated with an MTT assay at days 1, 3, 5, 7 and 9 (Figure 1F). Similarly, they were positive for the MSC surface

Preprints (www.preprints.org) | NOT PEER-REVIEWED | Posted: 4 April 2017 doi:10.20944/preprints201704.0016.v1

Peer-reviewed version available at Int. J. Mol. Sci. 2017, 18, , 1076; doi:10.3390/ijms18051076

markers, CD29, CD90, CD146 and STRO-1, but negative for the hematopoietic and endothelial surface markers, CD45, CD31 and CD34 (Figure 1G).

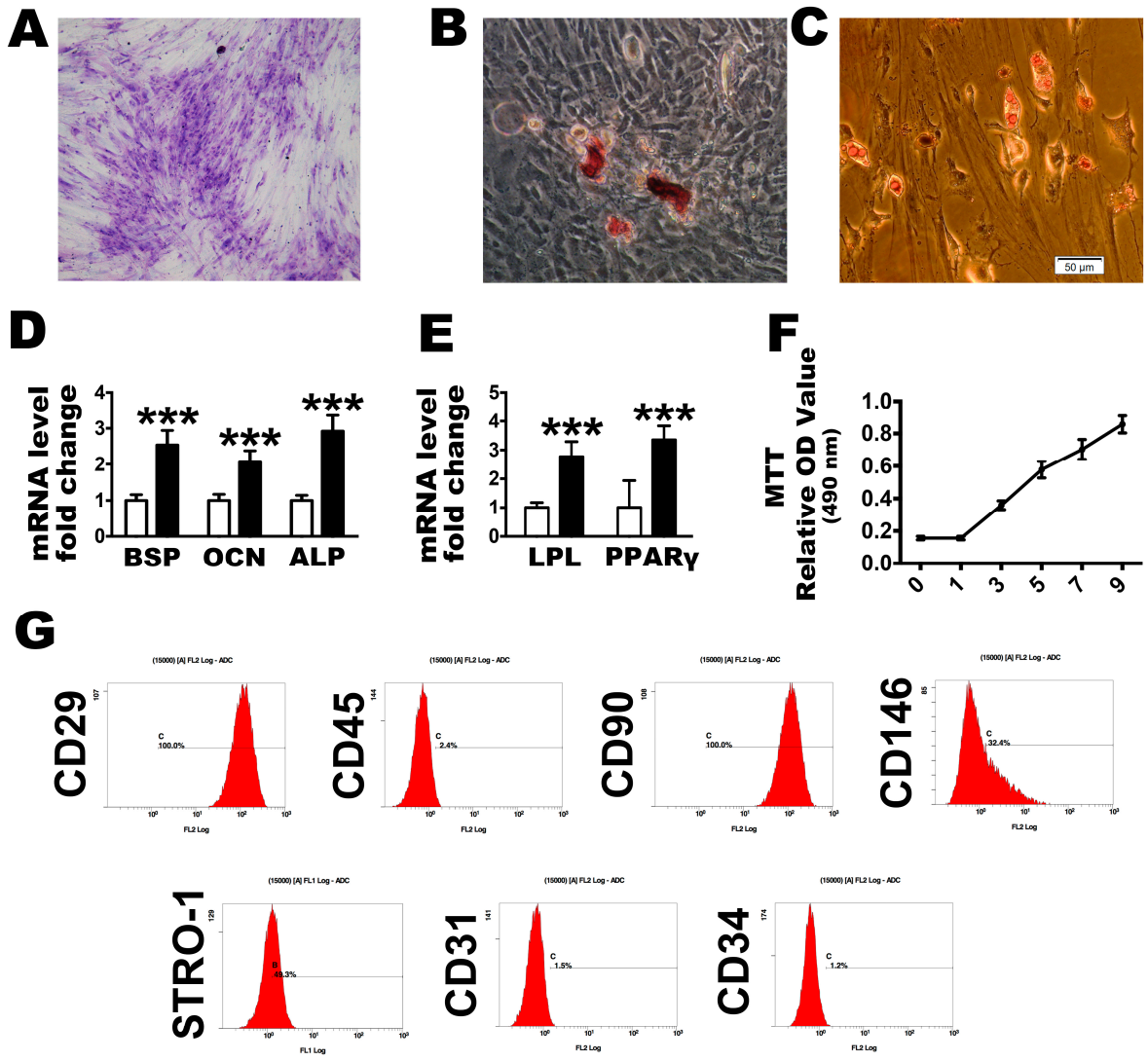

Figure 1. Identification of human PDLSCs. Representative image of colony-forming units and a random single-cell clone (A) on day 14. Representative images of mineralized cell nodules (B) following a 21-day osteogenic induction period and lipid droplets (C) following a 14-day adipogenic induction period. Bars = 50 μm. Osteogenesis (D) and adipogenesis (E) mRNA expression after condition culture. Proliferation of locally isolated PDLSCs, as assessed by MTT assays (F). Cell surface markers identified by flow cytometric analysis (G). The data are expressed as the mean ± SD. n=5. ***P < 0.001 represent significant differences between the indicated columns.

2. H_2O_2 stimulation leads to OS and Nrf2 signaling changes

In vitro, we stimulated human PDLSCs with a gradient of H_2O_2 concentrations to simulate OS in the gingiva and supporting connective tissue micro-environment *in vivo*

Preprints (www.preprints.org) | NOT PEER-REVIEWED | Posted: 4 April 2017 doi:10.20944/preprints201704.0016.v1

Peer-reviewed version available at Int. J. Mol. Sci. 2017, 18, , 1076; doi:10.3390/ijms18051076

during periodontitis. After exposure to 125, 250, 500 or 1000 μmol/L of H_2O_2 for 2 hours, the effect of OS model with different concentrations was investigated with an MTT assay, which revealed that cytotoxicity positively correlated with low to high H_2O_2 concentrations (Figure 2). The 1000 μmol/L concentration was the most severely cytotoxic to the cells. After OS was established on the PDLSCs, molecular OS and ROS markers, which have important roles in cell signaling and damage were analyzed with a fluorogenic assay that manifested that the ROS activation level was significantly elevated at all stimulation concentrations with increasing OS levels. Similar results were found in the expression of MDA (Figure 3A and B). However, regarding the phase II detoxifying enzymes, the SOD and GSH-Px levels were not decreased after exposure, but they were increased (Figure 3C and D). Additionally, the basal Nrf2 mRNA and protein expression levels were significantly upregulated (Figure 3E, I and J). The mRNA and protein levels of HO-1, NQO1 and γ-GCS, which are downstream of Nrf2, were 2-fold increased with the exposure concentrations (Figure 3F-J). These results indicate that the OS reaction was obvious because the oxidative and anti-oxidative molecules increased after H_2O_2 exposure and the anti-oxidative signaling of Nrf2 was activated.

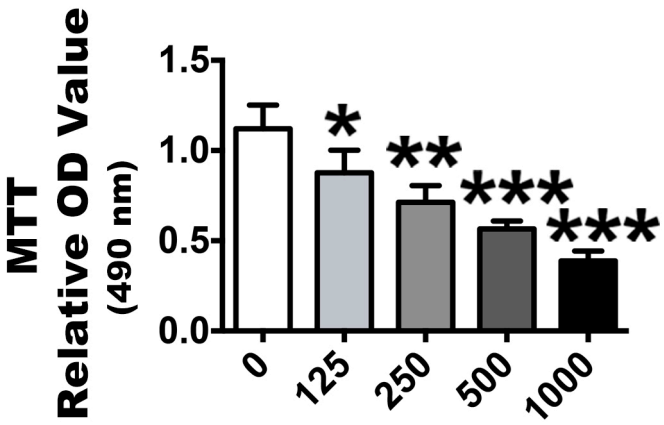

Figure 2. Proliferation of locally isolated PDLSCs after H_2O_2 stimulation, as assessed by MTT assays. The columns represent the mean values with SD. n=5. Different H_2O_2 concentration treatments containing 125 μmol/L, 250 μmol/L, 500 μmol/L and 1000 μmol/L, compared with a 0 μmol/L control group. *P < 0.05 **P < 0.01 and ***P < 0.001 represent significant differences between the indicated columns.

Preprints (www.preprints.org) | NOT PEER-REVIEWED | Posted: 4 April 2017 doi:10.20944/preprints201704.0016.v1

Peer-reviewed version available at Int. J. Mol. Sci. 2017, 18, , 1076; doi:10.3390/ijms18051076

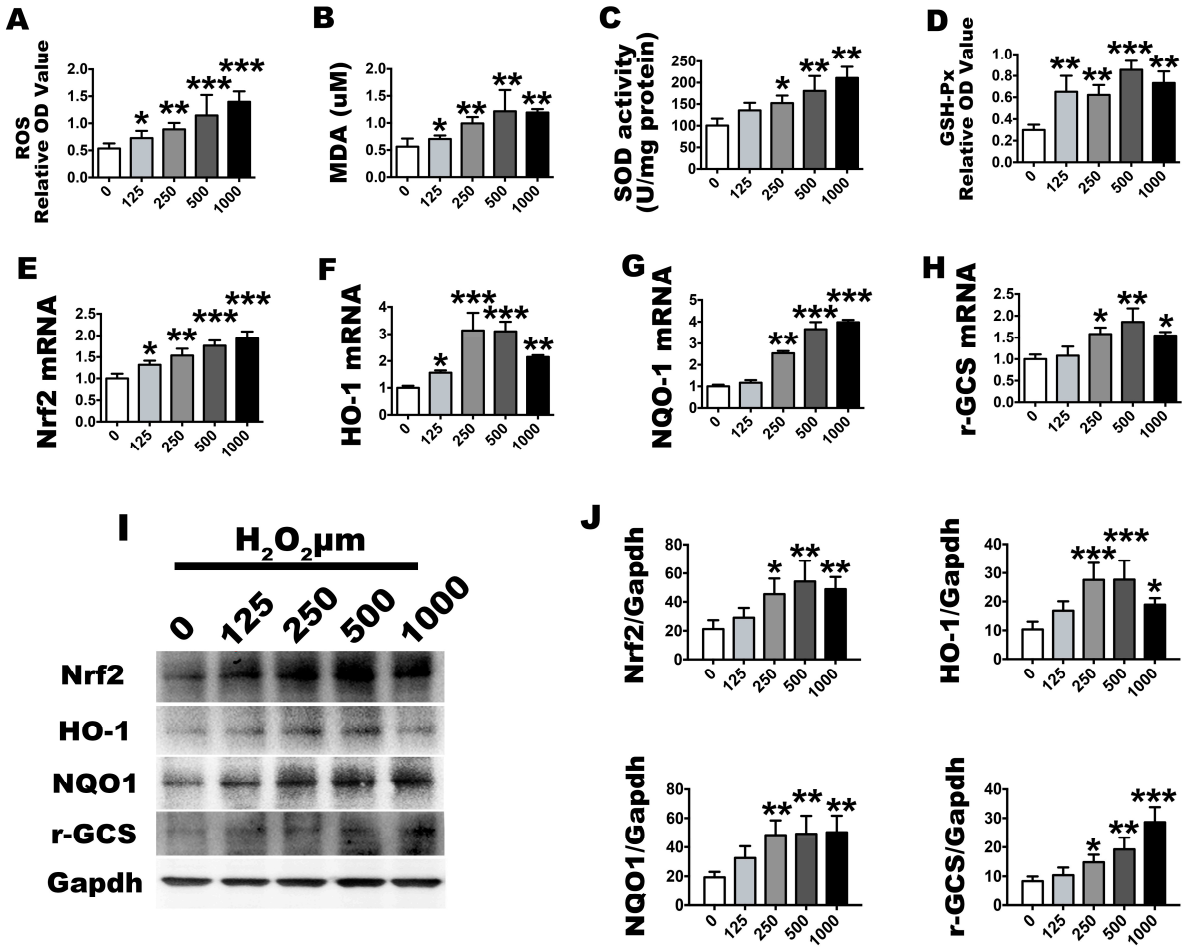

Figure 3. Effects of the H_2O_2 treatment model, as described in the group design, on cell oxidative stress and anti-oxidative changes. The corresponding ROS level were assessed by absorbance OD values (A), MDA expression levels (B) and SOD and GSH-Px absorbance OD values (C and D). Relative Nrf2, HO-1, NQO1 and γ-GCS (F-H) molecular gene expression levels, as determined by real-time PCR analysis. Western blot images for Nrf2, HO-1, NQO1 and γ-GCS (I) and their quantification (J). Data are presented as the means ± SD. n=5. Different H_2O_2 concentration treatments containing 125 μmol/L, 250 μmol/L, 500 μmol/L and 1000 μmol/L compared with a 0 μmol/L control group. *P < 0.05 **P < 0.01 and ***P < 0.001 represent significant differences between the indicated columns.

3. OS induces PDLSC apoptosis

Because sublethal H_2O_2 concentrations can directly or indirectly produce damage to nucleic acids and cellular proteins, we next evaluated the extent of apoptosis by TUNEL staining, fluorogenic assay, RT-PCR and western blotting to identify the effect of the OS microenvironment on PDLSCs. TUNEL staining indicated that with the oxide stimulation augmentation in the microenvironment the TUNEL-positive cells were significantly increased compared with the control group, and the highest positive rate was observed in the 1000 μmol/L group (Figure 4A and B). The PCNA and Ki67 mRNA levels, a main proliferation indicator, were significantly down-regulated in the 125 to 1000 μmol/L concentrations (Figure 4C). The caspase-3 and -9 mRNA expression levels were

Preprints (www.preprints.org) | NOT PEER-REVIEWED | Posted: 4 April 2017 doi:10.20944/preprints201704.0016.v1

Peer-reviewed version available at Int. J. Mol. Sci. 2017, 18, , 1076; doi:10.3390/ijms18051076

up-regulated at all concentrations. However, no up-regulation was detected in the mRNA expression level of caspase-8. Furthermore, similar to the gene expression levels, the fluorogenic analysis indicated that the active caspase-9 and -3 levels were increased following exposure; however, the active caspase-8 level was not increased (Figure 4D). The mRNA levels of the anti-apoptosis molecule, Bcl-2, was down-regulated; on the contrary, the mRNA levels of the apoptosis promoting molecules, Bax and c-fos, were up-regulated. The Bcl-2 and Bax western blot results were consistent with the mRNA level changes (Figure 3E and F). These findings suggest that the apoptosis levels increased gradually with the augmented oxidative stress and that the enhanced antioxidant effect could not protect against the apoptosis.

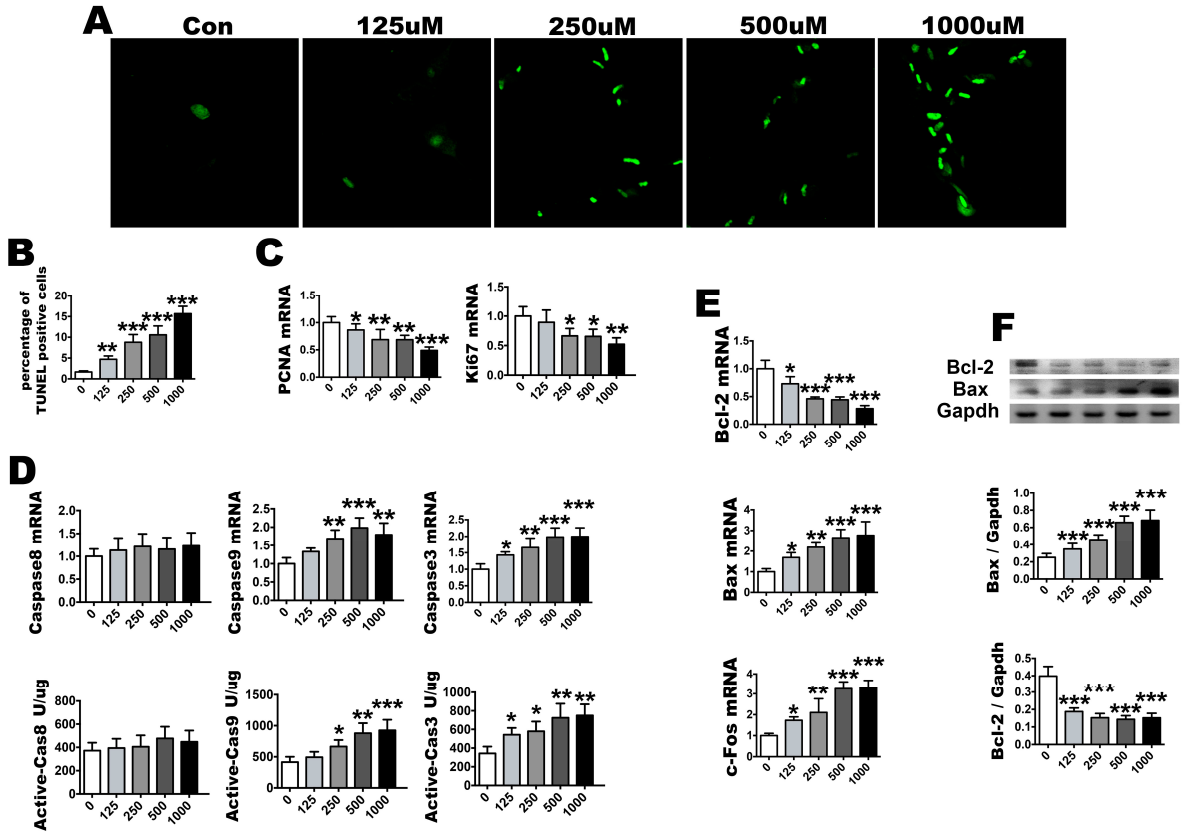

Figure 4. After H_2O_2 treatment, identification of cell proliferation and apoptosis. Representative cell apoptosis images, as assayed by TUNEL staining (A) and its quantification (B). Relative proliferation parameters of PCNA and Ki67, as determined by real-time PCR analysis (C). Caspase-8, caspase-9 and caspase-3 mRNA expression and active unit levels (D). Relative Bcl-2, Bax and c-Fos expression levels, as assayed by real-time PCR (E) and western blotting (F). Data are presented as the means ± SD. n=5. Different H_2O_2 concentration treatments containing 125 μmol/L, 250 μmol/L, 500 μmol/L and 1000 μmol/L compared with a 0 μmol/L control group. *P < 0.05 **P < 0.01 and ***P < 0.001 represent significant differences between the indicated columns.

Preprints (www.preprints.org) | NOT PEER-REVIEWED | Posted: 4 April 2017 doi:10.20944/preprints201704.0016.v1

Peer-reviewed version available at Int. J. Mol. Sci. 2017, 18, , 1076; doi:10.3390/ijms18051076

4. Nrf2 is a key molecule in PDLSC apoptosis protection during OS

To investigate the effect of Nrf2 on H_2O_2-induced apoptosis signaling cascades, Nrf2 silencing or overexpression through siRNA were used in PDLSCs (Figure 5A). After treatment with 1000 μmol/L H_2O_2, the mRNA of Nrf2 was up-regulated in the overexpression group and down-regulated in the silencing group, with no change observed in the negative control (Figure 5B, C and D). The same tendency was also observed because the mRNA and protein levels of NQO1, HO-1and γ-GCS, which are the downstream targets of Nrf2, were significantly consistent with this effect (Figure 5B, C and D). Furthermore, the up-regulated Nrf2 produced a significantly decreased TUNEL-positive cell rate (Figure 6A, B), caspase-9 and -3 mRNA levels and active caspase-9 and -3 units, but it had no effect on caspase-8 activation compared with the OS stimulation (Figure 6D). It also increased cell proliferation with the up-regulation mRNA of PCNA and Ki67 (Figure 6C). The anti-apoptosis ability of Nrf2 was revealed by up-regulating the mRNA and protein of Bcl-2 and down-regulating Bax and c-fos (Figure 6E and F). In contrast, silencing Nrf2 down-regulated proliferation, as demonstrated by PCNA and Ki67 mRNA expression, and it increased the TUNEL-positive cells and the caspase-9 and -3 activity but had no influenced on caspase-8. Finally, this silencing up-regulated the mRNA and protein expression levels of Bax and down-regulated Bcl-2 (Figure 6A-F). Overall, these results further corroborate the role of Nrf2 signaling in PDLSC anti-oxidative function improvement, as demonstrated by cell proliferation and anti-apoptosis enhancement, in H_2O_2-induced OS.

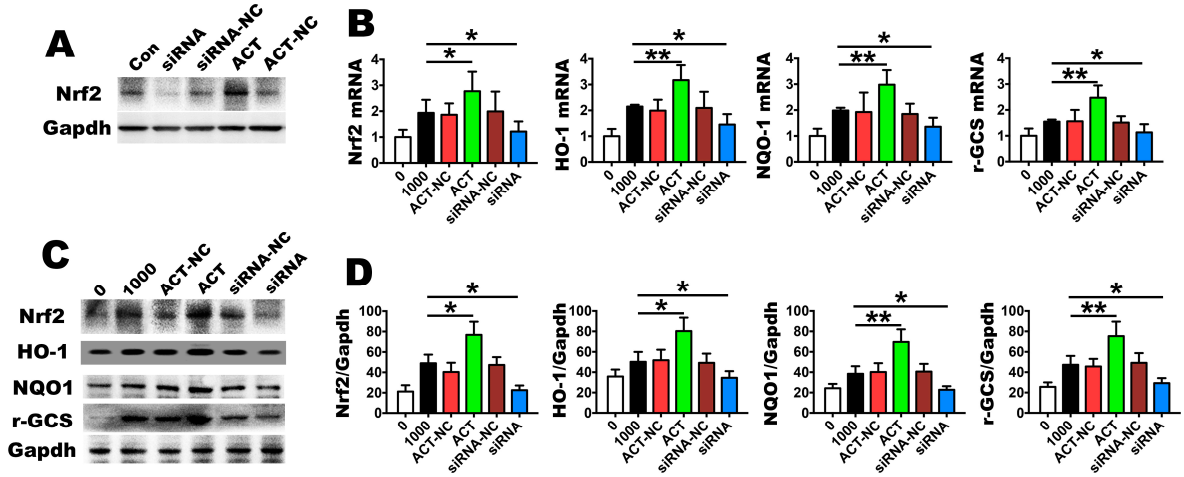

Figure 5. OS induced Nrf2 expression. The PDLSCs were treated with 1000 μmol/L H_2O_2 for 2 h. The PDLSCs were transfected with lentiviral Nrf2 for overexpression (ACT: activation) or a lentiviral control (ACT-NC: activation negative control), and they were silenced with Nrf2 siRNA (siRNA) or control siRNA (siRNA negative control). Overexpression or silence of Nrf2 expression levels were confirmed by western blot analysis (A) (n = 3). Relative gene expression levels of Nrf2 and its related downstream molecules, HO-1, NQO1 and γ-GCS (B), as determined by real-time PCR analysis. Western blot for the anti-oxidative molecules, Nrf2, HO-1, NQO1 and γ-GCS (C) and their

Preprints (www.preprints.org) | NOT PEER-REVIEWED | Posted: 4 April 2017 doi:10.20944/preprints201704.0016.v1

Peer-reviewed version available at Int. J. Mol. Sci. 2017, 18, , 1076; doi:10.3390/ijms18051076

quantification (D). Data are presented as the means ± SD. n=5. *P < 0.05 and **P < 0.01 represent significant differences between the indicated columns.

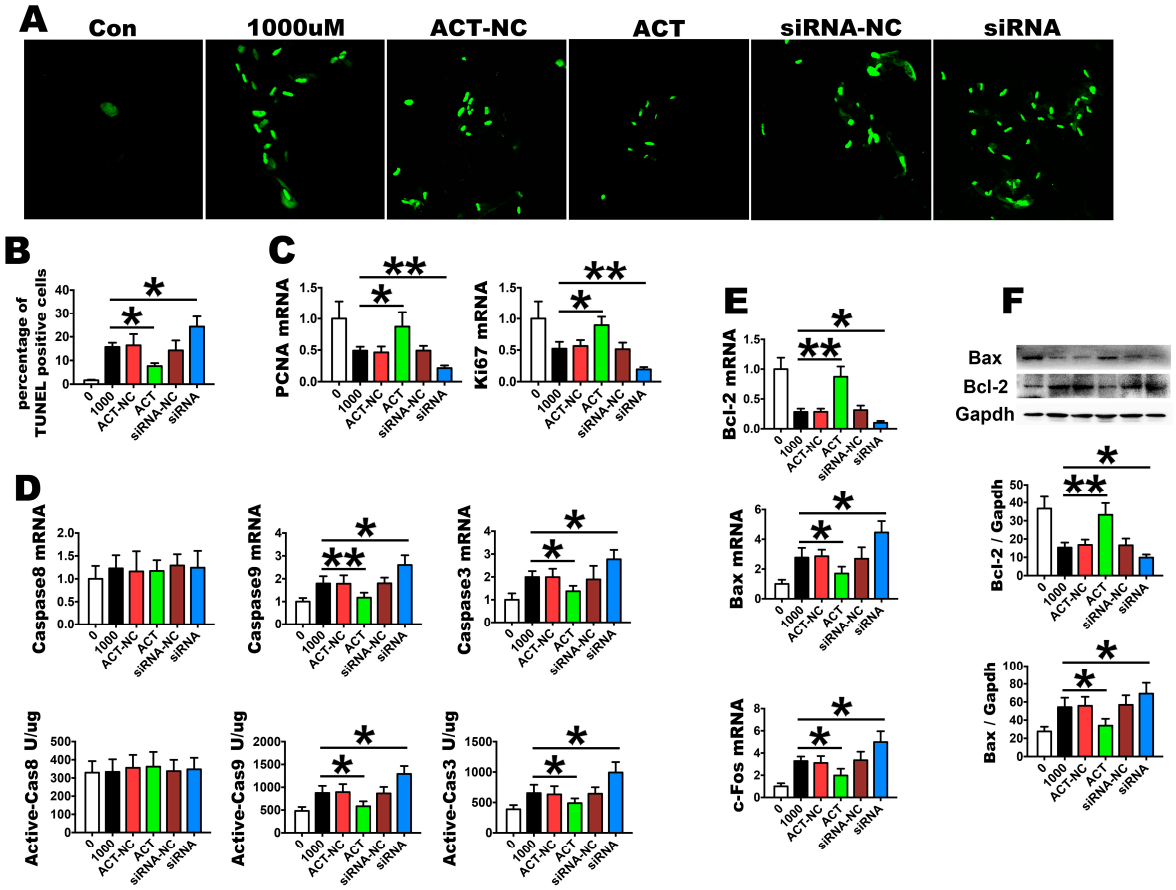

Figure 6. OS induced PDLSC apoptosis changes through Nrf2 overexpression or silencing. PDLSCs were treated with 1000 μmol/L H_2O_2 for 2 h. Representative cell apoptosis images, as assayed by TUNEL staining (A) and their quantification (B). Caspase-8, caspase-9 and caspase-3 mRNA expression and active unit levels (D). Expression levels of the relative apoptosis molecules, Bcl-2, Bax and c-Fos, as assayed by real-time PCR (E) and western blotting (F). Data are presented as the means ± SD. n=5. *P < 0.05 and **P < 0.01 represent significant differences between the indicated columns.

Discussion

Periodontal diseases are highly prevalent and are among the most common chronic disorders. They can affect up to 90% of the population and have plagued humans for centuries [24]. Research studies have indicated that partial oxidation of the micro-environment during periodontitis is an important reason for increased periodontal tissue damage [25]. Our previous studies found that the effect of bone defect repair using PDLSCs for periodontitis is negatively related to the degree of local oxidation in the micro-environment. This demonstrates that the oxidation environment is the main reason for the functional and repair ability of PDLSCs. In the present study, PDLSCs that were isolated from human teeth showed characteristics of MSCs that were positive for CD29,

CD90, CD146 and STRO-1 surface markers and negative for CD31, CD34 and CD45. We demonstrated that high-concentration H_2O_2 stimulation of PDLSCs led to a strong OS reaction with increased ROS and MDA, which was accompanied by a rise of anti-oxidant enzymes from PDLSCs, such as SOD and GSH-Px. This suggests that exposure to excessive H_2O_2 could imitate the micro-environment, in which PDLSCs are located in periodontitis patients.

DNA structure is an important target of ROS attack. Oxidative damage can directly lead to the rupture of DNA strands, locus mutation, and accelerate cell apoptosis [11, 26]. Apoptosis has two main pathways: the mitochondria and death receptor pathways [27, 28]. Fas is tumor necrosis factor receptor superfamily member. It is a transmembrane protein and, combined with FasL, can initiate death receptor apoptosis signal transduction, which plays a key role in the caspase cascade pathways [29]. Fas combines with FasL to format a death domain (DD), which contains a 60-70 amino acid sequence [30]. Because its N terminal contains a Fas-associated death domain (FADD) structure in the cytoplasm, which is called the death effect domain, its structure can activate the apoptosis signaling protease, caspase-8. Active caspase-8 can mediate its effects through caspase-3 to induce DNA degradation and cell apoptosis, including DNA breaks and chromosome condensation. Its formation in the nucleosome and concentrations in the cytoplasm complete the Fas mediated death receptor apoptosis pathway [31, 32]. Bax, a pro-apoptotic protein of the Bcl-2 family, is a key regulator of apoptosis. As reported in many apoptotic paradigms, Bax resides primarily in the cytosol of healthy cells, in an inactive state. In the mitochondria apoptosis pathway, Bax undergoes specific conformational changes, activates caspase-9 and cytochrome c leading to the activation of effector caspase-3 [33, 34]. In our results, caspase-3 activation, which has been shown to be up-regulated in TUNEL positive cells, revealed that OS could induce apoptosis in PDLSCs. The caspase-9, and not caspase-8, activation indicated that our H_2O_2-induced OS promoted the mitochondria apoptosis pathway and not the death receptor pathway.

Further, the oxidative or electrophilic modification of Keap1 or phosphorylation of serine 40 on Nrf2 by protein kinase C results in the stabilization and release of Nrf2 from Keap1. Nrf2 is the key factor in the cell oxidative stress reaction and is the central regulator of the cell oxidation reaction. In normal conditions, the organism uses a series of antioxidant systems and the expression of phase II detoxifying enzymes to remove excess ROS that contains SOD, GSH-Px, catalase and reduced glutathione (GSH) [35, 36]. In the body, the Nrf2/ARE signaling pathway acts as an important endogenous anti-oxidative stress pathway [37]. Under oxidative stress, Nrf2 binds to a DNA promoter and initiates the transcription of anti-oxidative genes that encode and modulate the expression of various antioxidant genes, enhances cellular resistance to oxidative stress, and thereby reduces damage to the body caused by oxidative stress. Wang *et al* demonstrated that Nrf2 is up-regulated in mesenchymal stem cells against starvation-induced mitochondrial dysfunction and apoptosis and that Nrf2 possibly mediates its protective effects as a part of the anti-oxidative pathway [38]. Our results showed that in PDLSCs, the Nrf2-mediated anti-oxidative signaling pathway was activated to clear excess free radicals by

up-regulating NQO1, HO-1 and γ-GCS mRNA and protein.

In recent years, accumulating evidence indicated that many drugs suppressed H_2O_2-induced oxidative stress and attenuated its induced cell injury via the expression of Nrf2 [39]. Research has also confirmed that Nrf2 itself influences the apoptosis inner and outer pathways at different levels [17]. Therefore, we believe that Nrf2 is extremely important in the process of cell apoptosis caused by oxidative stress. However, in our experiment, with an increasing concentration of H_2O_2, the Nrf2 antioxidant effect increased, as did the incidence of apoptosis. We suspect that the effect of Nrf2 on anti-apoptosis resistance was due to the factors under the PDLSCs state because apoptosis hid the anti-oxidation and anti-apoptosis effects of Nrf2. In this study, we executed Nrf2 overexpression, as a result Nrf2 effectively increased the level of antioxidant molecules, such as NQO1, HO-1 and γ-GCS, and increased cell proliferation by inducing PCNA and Ki67; at the same time, it effectively restrained the intrinsic apoptosis pathway. Recently, a study demonstrated that Nrf2 overexpression/ARE activation could protect cells against apoptosis through anti-oxidation [40]. In contrast, after silencing the Nrf2 expression levels, we found that the PDLSC anti-oxidant capacity was significantly decreased, the cell proliferation levels were decreased, and the intrinsic apoptosis pathway was up-regulated. This agrees with the results of Kubben [41], who found that repression of the Nrf2-mediated anti-oxidative response was a key contributor to MSC apoptosis and a premature aging phenotype. This proves that Nrf2 in PDLSCs plays a core anti-oxidant effect role and that it can inhibit the intrinsic apoptotic pathway by inhibiting active caspase-9 and Bax. Therefore, inhibiting PDLSC apoptosis plays a role in maintaining cell status and physiological functions.

In conclusion, in the present study, we successfully simulated oxidative stress in PDLSCs, and we identified that treatment with H_2O_2 led to apoptosis. Nrf2 alleviates PDLSCs through its anti-oxidative and anti-intrinsic apoptosis effects and by activating anti-oxidative enzymes and suppression of caspase-9, -3 and Bax. By increasing the exogenous Nrf2 expression levels and strengthening its antioxidant ability, we can achieve success by realizing the optimization of seed cells, thereby improving periodontitis bone repair, which offers a new tissue engineering application strategy for PDLSCs.

Methods

Isolation and culture of human PDLSCs.

Healthy premolars, for orthodontic reasons, were pulled and isolated at the Dental Clinic of School of Stomatology, Fourth Military Medical University, Xi'an, China. All subjects gave their informed consent for inclusion before they participated in the study. All procedures were performed according to institutional guidelines in accordance with the Declaration of Helsinki and were approved by the Ethics Committee of the Fourth Military Medical University, School of Stomatology, and an informed consent form that agreed to the contribution of their teeth for research purposes was signed by all donors. After

repeatedly rinsing the root surface with PBS, the middle third of the root was scraped to slice the periodontal membrane with a #11 sterile knife. It was washed with PBS 3 times and centrifuged at 800 r/min for 5 minutes, and the supernatant was removed. After enzymatic digestion for 20 min with 0.25% parenzyme, the tissues were incubated for 1 h with 1 mg/ml type I collagenase (Gibco, America) in alpha Minimum Essential Medium (α-MEM) (HyClone, America) at 37°C. The isolated cells were collected by brief centrifugation and were then resuspended in α-MEM supplemented with 10% FBS, 50 mg/ml streptomycin and 50 units/ml penicillin (HyClone, America). The culture medium was completely replaced every 3 days to replenish the non-adherent cells. Once the PDLSC cultures reached approximately 80% confluence, the cells were dissociated using 0.5% trypsin solution and expanded to passage one before being used for further experiments.

Colony-forming and cell viability assay.

Passage three PDLSCs were pre-incubated and transferred to 10-cm-diameter culture dishes (1000 cells per dish). Then, the cells were cultured under normal conditions until day 14, the cells in the dishes were fixed in 4% paraformaldehyde for 10 min and stained with 0.2% crystal violet (Sigma-Aldrich) for 15 h. The cell colonies were subsequently observed under a stereomicroscope (Olympus). Cell viability was analyzed using the 3-(4,5-dimethylthiazol-2-yl)-2,5-diphenyltetrazolium bromide (MTT) method. Briefly, the passage three PDLSCs were cultured in 96-well culture plates and the cells were stained with 5 mg/ml MTT (Sigma-Aldrich) at days 1, 3, 5, 7 and 9. The media were then carefully aspirated, and 150 μl of dimethyl sulfoxide (DMSO) was added to solubilize the colored formazan product for 10 min. The optical density was read at 490 nm using a microplate reader (Floustar Optima; BMG Labtech, Ortenberg, Germany). The OS experimental cells were exposed to 125, 250, 500 and 1000 μM H_2O_2 for 2 h. Then, the cells were stained with 5 mg/ml MTT using the procedures described above.

Flow cytometry.

Passage three PDLSCs were suspended in 400 μl of PBS and incubated with each specific antibody. To evaluate surface markers, phycoerythrin (PE)-coupled antibodies against CD29, CD45, CD90 (12-0299, 12-9459 and 12-0909, respectively, eBioscience, United States), CD31, CD34, CD146 and STRO-1 (ab9498, ab81289, ab75769 and ab102969, respectively, Abcam, United Kingdom) were used. The secondary antibodies used included Cy3-conjugated goat anti-rabbit IgG and FITC-conjugated goat anti-mouse IgG (Zhongshan Co. Ltd, China). After incubation for 30 min at 4 ˚C in the dark, the cells were washed with PBS and then resuspended in 400 μl of PBS. Cell fluorescence was determined using a FACS-Aria flow cytometer (BD Biosciences, San Jose, CA).

Detection of the multi-lineage differentiation ability of PDLSCs.

Passage three PDLSCs were plated on 6-well plates. To determine their osteogenesis abilities, after 24 hours, the cells were adhered, and the medium was switched to osteoinductive differentiation medium (HUXMA-90031, Cyagen Biosciences, America). The media were changed every two days. After osteogenic induction for 21 days, mineral nodules were detected by using alizarin red staining. To determine their adipogenesis abilities, passage three PDLSCs were adhered onto 6-well plates, and adipogenic induction medium (HUXMA-90021, Cyagen Biosciences, America) was used in place of the original culture medium. The medium was changed every two days. After 14 days, the lipid droplets were stained with Oil Red O solution.

Establishment of an oxidative stress model and determinations

Passage three PDLSCs were planted at a density of 10^5 in 6-well culture plates. After the cells were completely adherent, H_2O_2 was added to the media for final concentrations of 125 μmol/L, 250 μmol/L, 500 μmol/L and 1000 μmol/L to simulate the periodontitis environment as *in vitro* model of oxidative stress. After culturing for 2 h, the medium with H_2O_2 was removed, and the plates were rinsed with PBS three times for subsequent experiments. Non-H_2O_2 treated culture cells were utilized as a control group. ROS, SOD, MDA and GSH-Px levels were measured by fluorogenic assay to demonstrate the peroxidation level.

RNA transfection

PDLSCs that were grown to 50% confluence in a six-well plate were transfected with Nrf2 siRNA or an activation sequence using a lentiviral transfection reagent (Invitrogen) according to the manufacturer's instructions. The cells were then incubated for 6 h at 37°C in a CO^2 incubator. Then, the transfection mixture was replaced with DMEM-F12 that contained 10% FBS. All of the experiments were carried out 48 h after transfection. The lentiviral transfection efficiency was measured by confocal fluorescence. Nrf2 knockdown or activation was confirmed by protein expression measurements via western blotting.

Fluorogenic assay

Changes in intracellular ROS, MDA, SOD and GSH-Px levels were determined following the manufacturer's protocol with the Reactive Oxygen Species Assay Kit (S0033, Beyotime, China), Lipid Peroxidation MDA Assay Kit (S0131, Beyotime, China), Total Superoxide Dismutase Assay Kit (S0101, Beyotime, China) and Cellular Glutathione Peroxidase Assay Kit (S0056, Beyotime, China). The active caspase-3, -8 and -9 units were detected with Caspase 3, 8, 9 Activity Assay kits (C1116, C1152, C1158, Beyotime, China). To evaluate the caspase-3, -8, and -9, activities, isolated cells were homogenized in 100 μl

Preprints (www.preprints.org) | NOT PEER-REVIEWED | Posted: 4 April 2017 doi:10.20944/preprints201704.0016.v1

Peer-reviewed version available at Int. J. Mol. Sci. 2017, 18, , 1076; doi:10.3390/ijms18051076

of reaction buffer containing 2 mM Ac-DEVE-*p*NA, Ac-IETD-*p*NA and Ac-LEHD-*p*NA substrates, respectively, and were then incubated at 37°C for 2 h. Samples were measured with an ELISA reader at an absorbance of 530 nm for ROS, MDA and SOD, 412 nm for GSH-Px and at 405 nm for caspase-3, -8 and -9.

TUNEL staining

Apoptotic PDLSCs were assessed by TUNEL analysis with an *in situ* Cell Death Fluorescein Detection Kit (Roche) following the manufacturer's procedure. Briefly, after experimental stimulation, the cells were washed with PBS and fixed in 4% paraformaldehyde for 15 min. After rinsing with PBS, the cells were incubated with a reaction mixture solution for 30 min at 37°C in dark. Then, they were mounted and analyzed under a confocal laser scanning fluorescence microscope (BX-60, Olympus, Tokyo, Japan). Positive and negative controls were treated with 0.1 mg/ml pancreatic DNase I (F. Hoffmann-La Roche Ltd., Diagnostics Division) or labeling, respectively.

RNA extraction and reverse transcriptase PCR.

Total RNA was extracted from cells using Tripure (Roche, Swiss) according to the manufacturer's procedure. Reverse-transcription (RT)-PCR was performed using oligo deoxythymidine primers (Roche Diagnostics, Mannheim, Swiss) in 20 μl volumes at 42°C for 60 min. The RT-PCR reaction was conducted with 1 μg of total RNA, 1 μl of 20 μM oligo dT primer, and 18 μl of reaction mixture with AccuPower RT-PCR PreMix (Bioneer, Daejeon, Korea). Then, quantitative real-time PCR (qRT-PCR) was performed in a 20 μl total mixture volume for 39 cycles at 95°C for 30 s, 55°C for 30 s, and 72°C for 1 min. The primer sequences are detailed in **Table 1**.

Table 1. Gene primers

Genes	Forward primer	Reverse primer
BSP	GGCCACGATATTATCTTTACAAGCA	TCAGCCTCAGAGTCTTCATCTTCA
OPG	CTGCAGTACGTCAAGCAGGAGTG	TTTGCAAACTGTATTTCGCTCTGG
LPL	CCAAACTGGTGGGACAGGATG	GCTCCAAGGCTGTATCCCAAGA
PPAR-γ	TGGAATTAGATGACAGCGACTTGG	TTGAATGTCTTCAATGGGCTTCAC
PCNA	GGCCGAAGATAACGCGGATAC	GGCATATACGTGCAAATTCACCA
Ki67	TGGGTCTGTTATTGATGAGCC	TGACTTCCTTCCATTCTGAAGAC
Bax	ACGGAATACGACCACCGTGAACAGT TGCTG	TACTGCCTTTACTGGTGGTGGTATAGAT TCT
Bcl-2	CATGTGTGTGGAGAGCGTCAA	GCCGGTTCAGGTACTCAGTCA
c-Fos	TCTTACTACCACTCACCCGCAGAC	GGAATGAAGTTGGCACTGGAGAC
Fas	CGGGACCTCAGAGATGCTGGCTCTG CATG	GTGCCAGAGATAAGGCTCCCTGAATGC AC
Caspase3	GACTCTGGAATATCCCTGGACAACA	AGGTTTGCTGCATCGACATCTG

TRF1	TTGTTGAACCCTGCCACATTTA	CAGGGTTGAGGTCAGCCTACAGA
TRF2	ACCCAGGTTGATGACAGACCAG	AGATGTTGACAGCAAATGCCAAG
Nrf2	GATTCTGACTCCGGCATTTC	TCCCCAGAAGAATGTACTGG
NQO1	GGATTGGACCGAGCTGGAA	GAAACACCCAGCCGTCAGCTA
HO-1	TTGCCAGTGCCACCAAGTTC	TCAGCAGCTCCTGCAACTCC
γ -GCS	GAAGATGGTGATGGGATTTC	TTAGACAGTAGGTTGCTCC
GAPDH	GCACCGTCAAGGCTGAGAAC	TGGTGAAGACGCCAGTGGA

Western blotting.

Treated cells were washed with PBS and cytosolic protein extracts were prepared using Tripure (Roche, Swiss) with a protease inhibitor cocktail and 1% SDS. Protein concentrations were determined using the Bradford assay (Bio-Rad, CA, USA) according to the manufacturer's protocol. Protein lysate aliquots were separated on sodium dodecyl sulfate–10% polyacrylamide gels, and western blotting was performed. The proteins were transferred onto a 0.45 μm polyvinylidene difluoride (PVDF) membrane (Millipore, USA) in transfer buffer (20 mm Tris, 150 mm glycine, 20% methanol, pH 8.0) at 4°C and 100 V for 1 hour. The membrane was blocked with 5% non-fat milk in TBS-T for 1 hour at room temperature and incubated with primary antibodies and horseradish peroxidase (HRP)-conjugated IgG secondary antibodies. Protein bands were detected using an enhanced chemiluminescence (ECL) system (Bio-Rad, CA, USA).

Statistical analysis.

Data are expressed as the mean values and standard deviations (SD). SPSS 22.0 (SPSS Inc., IL, USA) was used for the statistical analysis and p values less than 0.05 were considered statistically significant for all statistical calculations. Normally, the data distribution was tested with the Shapiro-Wilk test with 95% confidence, and Levene's test was used to assess homogeneity of variance. One-way analysis of variance (ANOVA) was performed for multiple groups, and the Tukey's *post hoc* test was applied for comparisons between groups. All experiments were repeated at least three times.

Acknowledgements

This study was supported by grants from the National Natural Science Foundation of China No. 81500867 and No. 81400556.

Conflicts of interest

The authors declare no potential conflicts of interest with respect to the authorship and/or publication of this article.

Author Contributions

Yongjin Chen and Min Zhang conceived and designed the experiments; Yanli Liu and Hongxu Yang performed the experiments; Hongxu Yang and Yinhua Zhao analyzed the data; Hongxu Yang and Yanli Liu contributed reagents/materials/analysis tools; Yanli Liu wrote the paper.

Reference

1. Hajishengallis G. Periodontitis: from microbial immune subversion to systemic inflammation. Nat Rev Immunol. 2015;15(1):30-44.
2. Pihlstrom BL; Michalowicz BS; Johnson NW. Periodontal diseases. Lancet. 2005;366(9499):1809-20.
3. Ding G; Liu Y; Wang W; Wei F; Liu D; Fan Z; An Y; Zhang C; Wang S. Allogeneic periodontal ligament stem cell therapy for periodontitis in swine. Stem cells. 2010;28:1829-38.
4. Park CH; Rios HF; Jin Q; Sugai JV; Padial-Molina M; Taut AD; Flanagan CL; Hollister SJ; Giannobile WV. Tissue engineering bone-ligament complexes using fiber-guiding scaffolds. Biomaterials. 2012;33:137-45.
5. Zhu W; Liang M. Periodontal ligament stem cells: current status, concerns, and future prospects. Stem Cells Int. 2015;2015:972313.
6. Panjamurthy K; Manoharan S; Ramachandran CR. Lipid peroxidation and antioxidant status in patients with periodontitis. Cellular & molecular biology letters. 2005;10:255-64.
7. Kimura S; Yonemura T; Kaya H. Increased oxidative product formation by peripheral blood polymorphonuclear leukocytes in human periodontal diseases. Journal of periodontal research. 1993;28:197-203.
8. Waddington RJ; Moseley R; Embery G. Reactive oxygen species: a potential role in the pathogenesis of periodontal diseases. Oral diseases. 2000;6:138-51.
9. D'Aiuto F; Nibali L; Parkar M; Patel K; Suvan J; Donos N. Oxidative stress, systemic inflammation, and severe periodontitis. J Dent Res. 2010;89:1241-6.
10. Basu S; Helmersson J; Jarosinska D; Sallsten G; Mazzolai B; Barregard L. Regulatory factors of basal F(2)-isoprostane formation: population, age, gender and smoking habits in humans. Free radical research. 2009;43:85-91.
11. Kroemer G; Blomgren K. Mitochondrial cell death control in familial Parkinson disease. PLoS Biol. 2007;5:e206.
12. He Y; Jian CX; Zhang HY; Zhou Y; Wu X; Zhang G; Tan YH. Hypoxia enhances periodontal ligament stem cell proliferation via the MAPK signaling pathway. Genet Mol Res. 2016;15(4).
13. Granville DJ; Gottlieb RA. Mitochondria: regulators of cell death and survival. TheScientificWorldJournal. 2002;2:1569-78.
14. Sykiotis GP; Habeos IG; Samuelson AV; Bohmann D. The role of the antioxidant and longevity-promoting Nrf2 pathway in metabolic regulation. Current opinion in clinical

nutrition and metabolic care. 2011;14:41-8.
15. Pantano C; Reynaert NL; van der Vliet A; Janssen-Heininger YM. Redox-sensitive kinases of the nuclear factor-kappaB signaling pathway. Antioxidants & redox signaling. 2006;8:1791-806.
16. Grigsby B; Rodriguez-Rilo H; Khan K. Antioxidants and chronic pancreatitis: theory of oxidative stress and trials of antioxidant therapy. Digestive diseases and sciences. 2012;57:835-41.
17. Cao Y; Liu Z; Xie Y; Hu J; Wang H; Fan Z; Zhang C; Wang J; Wu CT; Wang S. Adenovirus-mediated transfer of hepatocyte growth factor gene to human dental pulp stem cells under good manufacturing practice improves their potential for periodontal regeneration in swine. Stem Cell Res Ther. 2015;6:249.
18. Motohashi H; Katsuoka F; Engel JD; Yamamoto M. Small Maf proteins serve as transcriptional cofactors for keratinocyte differentiation in the Keap1-Nrf2 regulatory pathway. Proceedings of the National Academy of Sciences of the United States of America. 2004;101:6379-84.
19. Lee JM; Johnson JA. An important role of Nrf2-ARE pathway in the cellular defense mechanism. Journal of biochemistry and molecular biology. 2004;37:139-43.
20. Haines DD; Lekli I; Teissier P; Bak I; Tosaki A. Role of haeme oxygenase-1 in resolution of oxidative stress-related pathologies: focus on cardiovascular, lung, neurological and kidney disorders. Acta Physiol (Oxf). 2012;204:487-501.
21. Joseph P; Jaiswal AK. NAD(P)H:quinone oxidoreductase1 (DT diaphorase) specifically prevents the formation of benzo[a]pyrene quinone-DNA adducts generated by cytochrome P4501A1 and P450 reductase. Proceedings of the National Academy of Sciences of the United States of America. 1994;91:8413-7.
22. Gebicki JM; Nauser T; Domazou A; Steinmann D; Bounds PL; Koppenol WH. Reduction of protein radicals by GSH and ascorbate: potential biological significance. Amino Acids. 2010;39:1131-7.
23. Mulcahy RT; Wartman MA; Bailey HH; Gipp JJ. Constitutive and beta-naphthoflavone-induced expression of the human gamma-glutamylcysteine synthetase heavy subunit gene is regulated by a distal antioxidant response element/TRE sequence. The Journal of biological chemistry. 1997;272:7445-54.
24. Pihlstrom BL; Michalowicz BS; Johnson NW. Periodontal diseases. Lancet. 2005;366(9499):1809-20.
25. Waddington RJ; Moseley R; Embery G. Reactive oxygen species: a potential role in the pathogenesis of periodontal diseases. Oral diseases. 2000;6:138-51.
26. Green DR; Kroemer G. The pathophysiology of mitochondrial cell death. Science. 2004;305:626-9.
27. Krammer PH. CD95's deadly mission in the immune system. Nature. 2000; 407: 789-95.
28. Ashkenazi A; Dixit VM. Death receptors: signaling and modulation. Science. 1998; 281: 1305-8.
29. Hu R; Du Q; Yin X; Li J; Wang T; Zhang L. Agonist antibody activates death receptor 6

downstream signaling involving TRADD recruitment. FEBS letters. 2014;588:401-7.
30. Lindsay J; Esposti MD; Gilmore AP. Bcl-2 proteins and mitochondria--specificity in membrane targeting for death. Biochimica et biophysica acta. 2011;1813:532-9.
31. Ashkenazi A; Dixit VM. Death receptors: signaling and modulation. Science. 1998;281:1305-8.
32. Henkler F; Behrle E; Dennehy KM; Wicovsky A; Peters N; Warnke C; Pfizenmaier K; Wajant H. The extracellular domains of FasL and Fas are sufficient for the formation of supramolecular FasL-Fas clusters of high stability. The Journal of cell biology. 2005;168:1087-98.
33. Ola MS; Nawaz M; Ahsan H. Role of Bcl-2 family proteins and caspases in the regulation of apoptosis. Molecular and cellular biochemistry. 2011;351:41-58.
34. Martinou JC; Youle RJ. Mitochondria in apoptosis: Bcl-2 family members and mitochondrial dynamics. Developmental cell. 2011;21:92-101.
35. Leonard MO; Kieran NE; Howell K; Burne MJ; Varadarajan R; Dhakshinamoorthy S. Reoxygenation-specific activation of the antioxidant transcription factor Nrf2 mediates cytoprotective gene expression in ischemia-reperfusion injury. FASEB journal : official publication of the Federation of American Societies for Experimental Biology. 2006;20:2624-6.
36. Kwak MK; Wakabayashi N; Itoh K; Motohashi H; Yamamoto M; Kensler TW. Modulation of gene expression by cancer chemopreventive dithiolethiones through the Keap1-Nrf2 pathway. Identification of novel gene clusters for cell survival. The Journal of biological chemistry. 2003;278:8135-45.
37. Thimmulappa RK; Mai KH; Srisuma S; Kensler TW; Yamamoto M; Biswal S. Identification of Nrf2-regulated genes induced by the chemopreventive agent sulforaphane by oligonucleotide microarray. Cancer research. 2002;62:5196-203.
38. Wang S; Zhang C; Niyazi S; Zheng L; Li J; Zhang W; Xu M; Rong R; Yang C; Zhu T. A novel cytoprotective peptide protects mesenchymal stem cells against mitochondrial dysfunction and apoptosis induced by starvation via Nrf2/Sirt3/FoxO3a pathway. J Transl Med. 2017;15(1):33.
39. Huang W; Shang WL; Li DH; Wu WW; Hou SX. Simvastatin protects osteoblast against H2O2-induced oxidative damage via inhibiting the upregulation of Nox4. Mol Cell Biochem. 2012;360(1-2):71-77.
40. Zhaleh F; Amiri F; Mohammadzadeh-Vardin M; Bahadori M; Harati MD; Roudkenar MH; Saki S. Nuclear factor erythroid-2 related factor 2 overexpressed mesenchymal stem cells transplantation, improves renal function, decreases injuries markers and increases repair markers in glycerol-induced Acute kidney injury rats. Iran J Basic Med Sci. 2016;19(3):323-9.
41. Kubben N; Zhang W; Wang L; Voss TC; Yang J; Qu J; Liu GH; Misteli T. Repression of the Antioxidant NRF2 Pathway in Premature Aging. Cell. 2016;165(6):1361-74.